



ISSN 1110-0451

## Arab Journal of Nuclear Sciences and Applications

Web site: [ajnsa.journals.ekb.eg](http://ajnsa.journals.ekb.eg)



(E S N S A)

### Potential activity of silver/hydroxyapatite nano composite against damaged liver in consequence to irradiation

Eman Ismail Abdel-Gawad<sup>1</sup>, Osama Ahmed Abbas<sup>\*1</sup>, Sameh A Awwad<sup>2</sup>

<sup>(1)</sup> Radioisotopes Department, Egyptian Atomic Energy Authority

<sup>(2)</sup> Department of Chemical Engineering, Higher Institute of Engineering & Technology, New Damietta, Egypt

#### ARTICLE INFO

Article history:

Received: 10<sup>th</sup> Jan. 2022

Accepted: 20<sup>th</sup> Mar. 2022

Keywords:

nano-Silver;

nano-Hydroxyapatite;

Radiation;

Hepatocellular Injury;

DNA damage, liver function;

Inflammatory Markers.

#### ABSTRACT

A silver/hydroxyapatite nanocomposite (nAg/HAp) has been formulated by a chemical route and characterized by X-ray analysis spectroscopy, Scanning Electron Microscope, Transmission Electron Microscope. The current study deals with assessing the efficiency of nAg/HAp against whole body  $\gamma$ -irradiation induced hepatic damage. Twenty-four male rats were assorted into three groups; one group was left as control while the rest two groups were subjected to 8 Gy single dose  $\gamma$ -ray and then treated by an intravenous injection (i.v.) with saline to one group and nAg/HAp solution to the other one. DNA damage and biochemical analyses for hepatic tissue and serum including liver function enzymes, antioxidant enzymes and inflammatory markers were evaluated. Histopathological examination was performed to verify the reached biochemical analyses outcomes. The experimental results depicted that i.v. nAg/HAp repaired the damage DNA induced by irradiation and this improvement confirmed by decrease in the concentration of 8-hydroxy-deoxyguanosine (8-OHdG) and caspase-3 as well as elevation of the antioxidant enzymes in the hepatic tissue. On the other hand, nAg/HAp significantly recovered serum liver enzymes (AST, ALT, and LDH) total bilirubin (TB) and albumin as well as decreased the levels of MCP-1, IL-6, IL-10, TNF- $\alpha$  and MMP-9. Histopathological examinations exhibited the ability of nAg/HAp in overcoming the damage consequent to irradiation and recovered the hepatic cellular structure for nAg/HAp group with minor change represented by diffusion of some inflammatory cells in between hepatocytes. It can be concluded that nAg/HAp offers a promising treatment against hepatocellular injury induced by  $\gamma$ -irradiation.

#### INTRODUCTION

Silver nanoparticles (nAg) have wide biomedical applications due to their natural antimicrobial and fungicidal activity [1]. The distinctive physicochemical properties of nAg gave them a great importance in the production of many medical tools and materials and in a diverse range of consumer products [2,3].

Although nAg has proven merit as a drug in various medical fields, its clinical use is limited due to its toxic effect [4]. The cytotoxicity evidences of nAg depended on *in-vitro* studies, which is the biological conditions that are extremely different from *in-vivo* conditions of living system. The agglomeration and dissolution in biological media are dependent on the method of nAg preparation. In the biological media, the surface of nAg oxidize and release Ag<sup>+</sup> which have the strong affinity to interact with sulfur containing macromolecules and

induce apoptosis mediated ROS and mitochondrial pathway [5]. To avoid this disadvantage, nAg formulation requires to support on the surface of different substrates [6]. However, several methods have been developed for nAg synthesis for the purpose of control of the particles morphology and the physicochemical properties to appropriate the practical applications [7]. However, nanocomposite of Ag and HAp (nAg/HAp) have potential medical applications because nHAp is an inorganic component of hard tissue and has better bioactivity and nAg has antitoxical properties [8].

Ionizing radiation hazardous effect on human health is well documented. Exposure to a large single dose of radiation tends to cause injury more than the same dose given for a prolonged period. The energy emitted from ionizing radiation is sufficient to damage the cellular components including DNA, proteins and cellular

membrane [9]. The oxidative stress spreads in a wide range with the assistance of intracellular communication mechanisms. The main mechanism of the radiation is the interaction with water in the biological media, and the generation of excessive ROS. Consequence events of ROS are depletion in antioxidant system, augmentation of inflammatory cytokines, inhibition of immunity, induction of apoptosis and cancer. However, the cells are extremely efficient in repairing the damage within the limits of their capacity. If the cells damage is not properly repaired, it can lead to cellular death or harmful changes in the DNA with prospect a mutation [10].

Because the radiotherapy has fatal effects on healthy cells, there is a growing interest in finding the therapeutic agents for human health. The current study aimed to formulate a biosafe Ag/HAp nanocomposite by the simple method to employ as a therapy for the damaged liver of rats exposed to 8 Gy of whole body  $\gamma$ -irradiation. The efficiency of nanocomposite was investigated by hepatic genotoxicity test (Comet assay), hepatic histopathological examination and biochemical analyses including liver enzymes, cytokines and oxidant status.

## EXPERIMENTAL APPROACH

### *Chemicals used:*

The preparation of Ag/HAp nanocomposite was performed using the following pure chemicals and reagents: silver nitrate ( $\text{AgNO}_3$ , Mwt.169.88g/mole, Johnson Matthey), ammonium hydroxide ( $\text{NH}_4 \text{OH}$ , Mwt. 35.5g/mole, May & Baker, England), poly vinyl alcohol (PVAL) (Mwt. $\approx$ 160000 g/mole), anhydrous diammonium hydrogen orthophosphate ( $(\text{NH}_4)_2\text{HPO}_4$ , 132.06g/mole, S.D. Fine Chem. Ltd. Mumbai), calcium nitrate tetrahydrate ( $(\text{Ca}(\text{NO}_3)_2 \cdot 4\text{H}_2\text{O}$ , Mwt. 236.15g/mole, Merk, Germany), polyvinylpyrrolidone (PVP) and sodium hydroxide (NaOH). Deionized water was used in preparing the solutions. Lead nitrate was used as a solution in 0.9% saline.

### *Source of radiation:*

The source of radiation was provided from gamma cell-40, cesium-137 source with dose rate of 0.84 Gy  $\text{min}^{-1}$  is belonging to the National Center for Radiation Research and Technology (NCRRT), Cairo, Egypt.

### *Preparation of nAg/HAp:*

Nano-silver synthesized in nHAp structure to inhibit its toxicity by controlling the release of Ag ions. Nano Ag was prepared chelated by nHAp in polymeric matrix

route. HAp stands out because it is similar in structure and chemical composition to the mineral of hard tissue in the body. Other factors such as ionic strength, pH and the presence/absence of other salts were utilized to produce an advanced structure of nAg supported on the surface of HAp nanoparticles (nAg/HAp) with developed characteristics. Polyvinyl alcohol was dissolved in 500 ml warm deionized water at 70°C, a free complete evolved. Calcium nitrate was added and 0.005 gm of silver nitrate (1/5  $\text{LD}_{50}$ ), then ammonium hydrogen ortho phosphate was added with in a molar ratio of 1.67 to calcium nitrate under PH control. After the addition of ammonium orthophosphate, the crystal structure of HAp was formed and trapped Ag ions to declare its toxic inhibition. The formed gel was filtered and dried at 80°C for 24 hours.

### *Characterization of nAg/HAp:*

Sample of the nAg/HAp product was characterized using Energy-dispersive X-ray analysis spectroscopy (EDAX) using EDAX (Ametek), High-resolution transmission electron microscope (TEM) JEOL2100 and Scanning Electron Microscopy (SEM) Philips XL30 instrument made in Holland.

### *Determination of nAg/HAp $\text{LD}_{50}$ :*

To evaluate  $\text{LD}_{50}$  of nAg/HAp, eighteen rats weighted 160-170 gm were divided into equally six groups. They were injected intravenously once with different doses (100, 300, 600, 1200, 1600 and 2600 mg/kg b.w.). The physical activity and mortality of rats were followed up and at the end of experiment, dead rats were counted in each group. The  $\text{LD}_{50}$  value was calculated according to the method of Lorke [11]

$$\text{LD}_{50} = \text{M}_0 + \text{M}_1 / 2$$

$\text{M}_0$ = Highest dose of substance at which no mortality,  
 $\text{M}_1$ = Lowest dose of substance at which mortality.

### *Estimation of hepatotherapeutic effect of nAg/HAp:*

Histopathological examination and liver enzymes analysis were performed in each trial to select the optimal dose and design of the experiment. Irradiated rats were injected with nAg/HAp either as a single dose or as a fractionated dose at level of 75, 150 and 300 mg/kg b.w. Based on the obtained results and consistent with the previous study by [8], the best therapeutic effect of nAg/HAp was reported is 75 mg/kg b.w. weekly for 4 weeks.

**Animals:**

Twenty –four male rats weighing 160-170 gm b. w. were used in this study. The cages of the rats were placed in alternative light/dark cycle (12 hours for each) and suitable conditions of heat and humidity. Rats provided with food and water freely. The study was conducted in accordance with the Guide for the Care and Use of Laboratory Animals [12] and this protocol complied with the guidelines of the Ethical Committee at National Center for Radiation Research, Egyptian Atomic Energy Authority, Cairo, Egypt (NCRR-EAEA).

**Experimental design:**

Twenty-four rats were assorted into three equal groups: control group (injected intravenously 1 ml/rat normal saline once a week for three weeks, termed C group), irradiation model group (8 Gy whole body irradiation, termed IR group and injected normal saline 1 ml/rat once weekly for three weeks.), and nAg/HAp group (rats were received an intravenous injection of nAg/HAp at a dose level of 100 mg/kg/bw dissolved in 1ml saline once/week for three weeks on the next day of irradiation, termed IR+ nAg/HAp). Serum and tissues were collected after 24 hours of the last dose of nAg/HAp injection.

**Samples collection:**

Blood was collected from orbital vein and serum was taken after centrifugation at 3000 rpm for 10 min for biochemical analyses. Livers were removed out after rat's decapitation, washed by ice-cold saline and dried. Each liver was divided into 3 parts: two parts were put in saline and stored at  $-80^{\circ}\text{C}$  to evaluate the fragmentation of DNA and assayed some biochemical parameters. The third part was put in 10% formalin for the ; histopathological examination.

**Method of liver homogenization:**

To prepare 20% of liver homogenate; a piece of liver weighing 2 g was homogenized in saline phosphate buffer at pH = 7.4. The homogenate was centrifuged at 20 000 rpm for 20 min at  $4^{\circ}\text{C}$ . Then, the whole product was used for analysis [9].

**Genotoxicity test (Comet assay):**

The genotoxicity test was applied in different groups by comet assay technique to reveal the degree of DNA fragmentation. The comet assay was performed using a fluorescence microscope connected to a CCD camera with an image analysis system at 400 $\times$  magnification. This system acquired the images, calculated the intensity

for each cell, estimated the components of comet cell, and finally evaluated the ranges of the derived parameters. To evaluate the DNA damage, the comet tail length (TL), the percentage of fragmented DNA (tail DNA %), and the tail moment (TM) were determined. TL expresses the value of the fragmented DNA in micrometres and is measured from the cell center. The damage of DNA was quantified by determining the distance between the comet head and the tail.

**Biochemical analyses of the liver homogenate:**

In whole liver homogenate, 8-hydroxy-deoxyguanosine (8-OHdG) and caspase-3 levels were assessed based on a solid phase enzyme linked immunosorbent assay (ELISA) obtained from Life Sciences Advanced Technologies, Saint Petersburg FL 33710 and sandwich ELISA kits USCN Life Science, Rat caspase-3, Catalog no. E90626, China), respectively, according to the manufacturer's instructions. Determination of malondialdehyde (MDA) was evaluated according to the colorimetric method of Erdelmeier [13]. Superoxide dismutase (SOD), glutathione peroxidase (GPx) and catalase (CAT) were estimated according to the techniques of Janknegt [14], Paglia [15] and Aebi [16] respectively.

**Serum analyses:**

Aspartate aminotransferase (AST) and alanine aminotransferase (ALT) were evaluated according to the German Society for Clinical Chemistry [17]; lactate dehydrogenase (LDH) was evaluated by the kinetic method according to Vanderlinde [18]; and the extent of total bilirubin and serum albumin were analyzed based on full automated Siemens Dimension Clinical Chemistry System. Serum monocytes chemoattractant protein-1 (MCP-1), interleukin-6 (IL-6) and interleukin-10 (IL-10) were evaluated using ELISA kits purchased from MyBioSource (San Diego, CA, USA) Catalog no. MBS8804486, MBS4500393 and MBS2700945) respectively. The concentration of tumor necrosis factor- $\alpha$  (TNF- $\alpha$ ) was determined by Rat TNF-alpha ELISA Kit from MyBioSource (San Diego, CA, USA, Catalog no. MBS2507393). Metalloproteinase-9 (MMP-9) was assessed using sandwich ELISA kits (Rat MMP-9, Catalog no. E90553, China).

**Histopathological assessment:**

The liver tissue was fixed in 10% formal saline for twenty-four hours. Washing with tap water followed by dehydration treatment that was performed by applying a series of diluted alcohols. Specimens were purified by xylene and put in paraffin at  $56^{\circ}\text{C}$  in a hot air oven for

twenty-four hours. Paraffin–bees wax tissue blocks were prepared for 4  $\mu\text{m}$  sections which was cut using sliding microtome. The obtained tissue sections were collected on glass slides, deparaffinized, stained by hematoxylin & eosin stains and examined using light microscopy [19].

#### Statistics:

The values represented the average data for 8 rats ( $\pm$  SE). Data obtained were analyzed using a one-way analysis of variance (ANOVA). The level of significance between mean values was set at  $p \leq 0.05$ . All statistical analyses were performed using SPSS software (version 20.0).

## RESULTS

### Characterization of nAg/HAp:

SEM analysis showed that silver nano-particles had a nano size range from 75 to 80 nm and successfully dispersed in the nHAp (Fig.1a & 1b). EDAX analysis showed the percentage of nAg post- filtration and drying process, whereas the analysis of the filtered solution did not detect the silver or calcium ions (Fig.2). TEM showed the distribution of nAg on the nHAp as shown in figure (3a & 3 b). Ca/P was formed with molar ratio of 1.67. It was noticed that the presence of nAg did not affect the crystal structure of nHAp.

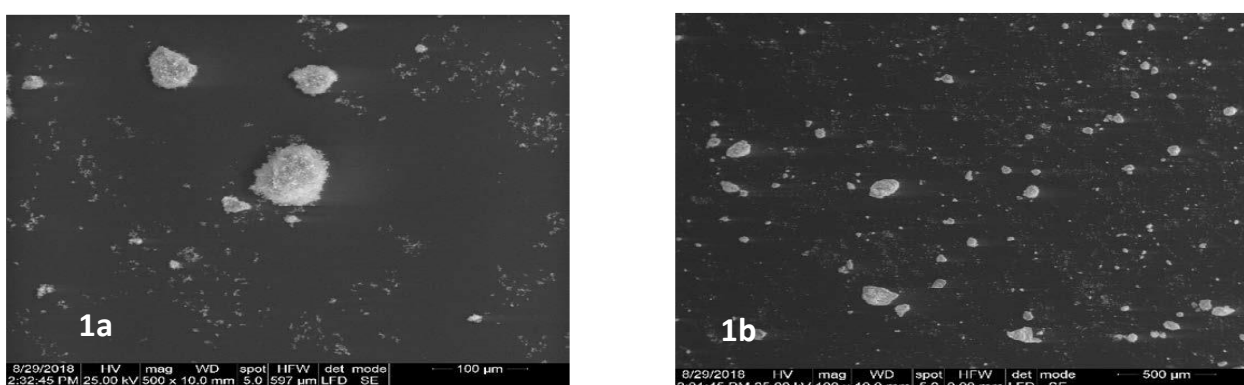


Fig. (1): SEM of dried nAg sample

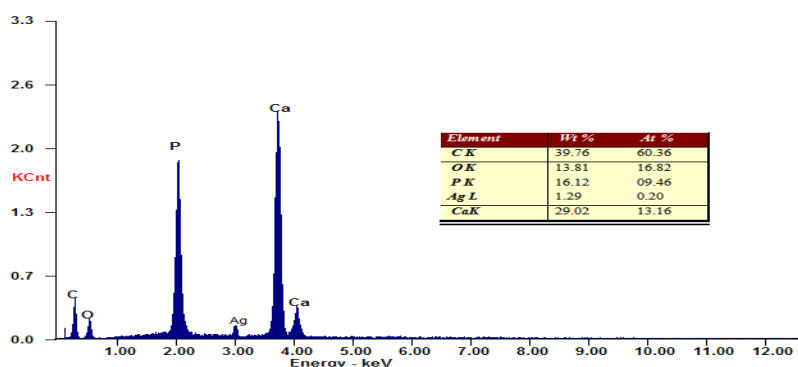
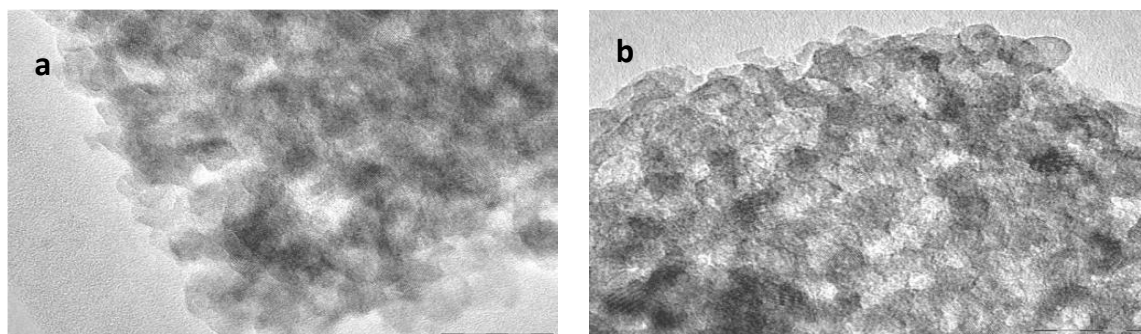


Fig. (2): EDAX analysis of dried nAg/Hap



(3a): Low concentration of nAg

(3b): High concentration of nAg

Fig. (3): TEM of the prepared nAg/HAp

### Liver morphological features:

Fig. (4) demonstrates the morphological features of liver in different groups. Irradiated liver appeared different from the control and irradiated-treated livers as regard to texture, color and size.

### Comet assay:

The comet assay is one of the most accurate techniques for the determination of an diverse types of DNA damage. The extent of DNA injury was

expressed by the stained DNA Tail length ( $\mu\text{m}$ ), Tailed % and Tail moment in unit (Table1). The single cell electrophoresis showed that the length of DNA comets tail of irradiated rats' hepatocytes was longer (Fig. 5 b) as compared with controls (Fig. 5a) indicating the adverse effect of irradiation on DNA. Rats that received an intravenous injection of nAg/HAp showed a reduction in their comets tail as shown in (Fig. 5c) indicating the positive role of nAg/HAp in repairing the fragmented DNA due to 8 Gy gamma irradiation exposure.



Fig. (4): photograph of morphological livers in different groups

Table (1): Score of hepatic DNA damage in the different rat groups

Parameters	Groups	C	IR	IR+nAg/HAp
Tailed %		4	16	7
Untailed %		96	84	93
Tail length ( $\mu\text{m}$ )		1.33	5.54	2.89
Tail DNA %		1.21	4.60	2.7
Tail moment UNIT		1.61	25.48	7.80

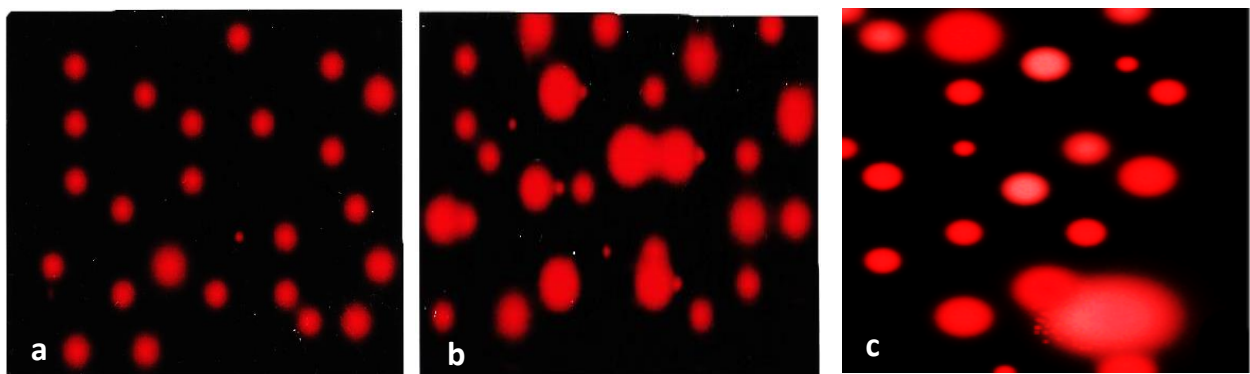


Fig. (5): Photomicrographs showed comet assay of rat's liver  
(5a) Group C, (5b) Group IR, (5c) Group IR+nAg/HAp



**Biochemical analysis results:**

The current results revealed that the 8-OHdG and caspase-3 were increased significantly ( $p < 0.05$ ) in the hepatic tissues of the IR group as compared to control and irradiated-treated groups. It was found that i.v. injection of nAg/HAp significantly reduced 8-OHdG and caspase-3 levels when compared with the IR group, this reduction did not reach the control levels (Table 2).

Regarding to irradiated rats, the hepatic MDA level was increased, while the SOD, GPx and CAT values were decreased ( $P < 0.05$ ) as compared to control rats. Reduction in the MDA value and augmentation in SOD, GPx and CAT activity ( $P < 0.05$ ) appeared in the IR+ nAg/HAp group when compared to IR group (table 3). The levels of SOD, GPx and CAT enzymes recorded insignificant differences between nAg/HAp and C groups.

The obtained results suggested that exposure to 8 Gy whole body  $\gamma$ -irradiation elevated the level of AST, ALT, LDH as well as TB and diminished Alb level in serum. Ag/HAp nanocomposite had a positive effect in diminishing the elevation of liver function markers when compared to IR group, but this neutralized impact did not reach the control level except for Alb concentration which recorded  $3.72 \pm 0.21$  g/100ml compared to  $4.83 \pm 0.57$  g/100 ml in C group (Table 4).

Compared to the control group: MCP-1, IL-6, TNF- $\alpha$  and MMP-9 levels were elevated while IL-10 level was diminished in the serum of the irradiated group ( $p < 0.05$ ). These immune markers were enhanced in the IR+ nAg/HAp group versus the irradiated group (at  $p < 0.05$ ). On the other hand, the values of IL-6, IL-10 and TNF- $\alpha$  content for the rats in irradiated-treated group showed non-significant changes as compared to the control group as indicated in Table (5).

**Table (2): Hepatic 8-OHDG and Caspase-3 in the different groups**

Groups	Parameters	8- OHDG (pg/mg)	Caspase-3 (ng/100g tissue)
C		159.34 <sup>a</sup> ±7.53	64.76 <sup>a</sup> ±0.99
IR		197.71 <sup>b</sup> ±5.97	138.33 <sup>b</sup> ±5.00
IR+nAg/HAp		171.31 <sup>c</sup> ±8.66	90.86 <sup>c</sup> ±2.32

Values are the mean  $\pm$  SE. Values in the same column mark by different letters are differ significantly ( $p < 0.05$ ).

**Table (3): Hepatic oxidative stress markers in the different groups**

Groups	C	IR	IR+nAg/HAp
MAD ( $\mu$ M/gm)	4.31 <sup>a</sup> ±0.73	11.98 <sup>b</sup> ±1.46	7.58 <sup>c</sup> ±0.98
SOD(U/mg protein)	491.82 <sup>a</sup> ±6.87	308.84 <sup>b</sup> ± 8.33	437.72 <sup>ac</sup> ±6.42
GPx(U/mg protein)	661.05 <sup>a</sup> ±5.74	450.27 <sup>b</sup> ± 5.99	595.78 <sup>ac</sup> ±6.76
CAT (U/mg protein)	42.33 <sup>a</sup> ±3.63	21.39 <sup>b</sup> ± 1.81	38.52 <sup>a</sup> ±2.85

Values are the mean  $\pm$  SE. Values in the same raw mark with different letters are differ significantly ( $p < 0.05$ ).

**Table (4): Serum liver function markers in the different groups**

Groups	C	IR	IR+nAg/HAp
AST(U/L)	187.73 <sup>a</sup> ±6.88	283.71 <sup>b</sup> ±6.32	210.77 <sup>c</sup> ±4.81
ALT (U/L)	148.84 <sup>a</sup> ±5.45	213.05 <sup>b</sup> ±4.67	186.11 <sup>c</sup> ±3.56
LDH (U/L)	780.64 <sup>a</sup> ±7.98	1217.44 <sup>bc</sup> ±7.22	950.43 <sup>d</sup> ±8.45
Alb (g/100ml)	4.83 <sup>a</sup> ± 0.57	2.36 <sup>c</sup> ±0.04	3.72 <sup>ab</sup> ±0.21
TB (mg/dL)	0.18 <sup>a</sup> ±0.21	0.62 <sup>b</sup> ±0.01	0.23 <sup>a</sup> ±0.01

Values are the mean  $\pm$  SE. Values in the same raw mark with different letters are differ significantly ( $p < 0.05$ ).

**Table (5): Serum cytokines in the different groups**

Groups	C	IR	IR+nAg/HAp
MCP-1 (pg/ml)	103.5 <sup>a</sup> ± 4.64	355.25 <sup>b</sup> ± 8.01	200.83 <sup>cd</sup> ±5.63
IL-6 (pg/ml)	337.69 <sup>a</sup> ±7.43	551.73 <sup>c</sup> ±5.68	423.28 <sup>ad</sup> ±8.32
IL-10 (pg/ml)	611.38 <sup>a</sup> ±9.39	385.28 <sup>b</sup> ±6.73	444.71 <sup>ac</sup> ±9.61
TNF- $\alpha$ (pg/ml)	23.44 <sup>a</sup> ± 1.71	44.92 <sup>b</sup> ±2.21	29.75 <sup>a</sup> ±2.73
MMP-9 ng/ml	2.33 <sup>a</sup> ±0.06	9.54 <sup>b</sup> ±1.11	5.85 <sup>c</sup> ±0.25

Values are the mean  $\pm$  SE. Values in the same raw mark with different letters are differ significantly ( $p < 0.05$ ).

### Histopathological results:

As shown in Figure (6), the hepatic tissue of the control group showed a normal structure with cords of hepatocytes radiating from the central vein (C.V) and separated by blood sinusoids (S). However, the liver section for the rats exposed to 8 Gy of irradiation showed extensive hepatic alterations including degeneration of parenchymal hepatocytes (d) and pyknotic hepatocytes (p) (Fig.7) as well as inflammatory cells in between the fatty changed hepatocytes (arrow) (Fig. 8) and in portal area (m) (Fig. 9) associated with dilatation and congestion in the central vein (C.V) with fatty change (f) and hydropic degeneration (arrow) in the hepatocytes (Fig.10). Administration of nAg/HAp post-irradiation restored the architecture of central vein (C.V) and surrounding hepatocytes (h) (Fig. 11) with few inflammatory cells diffused in between hepatocytes (m) as shown in Fig. (12).

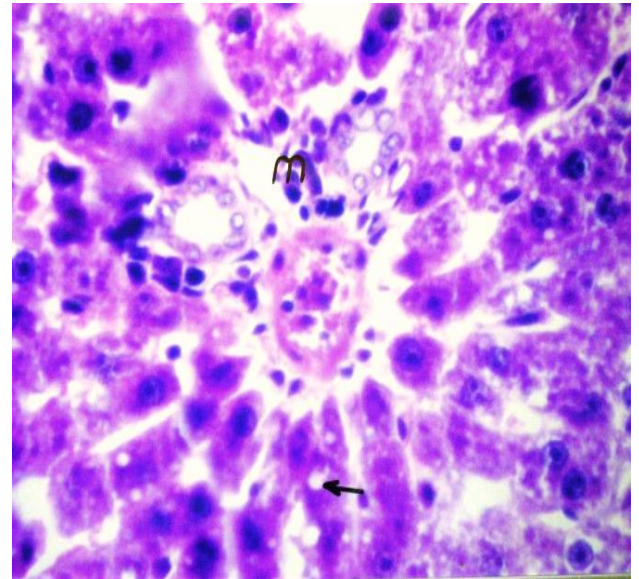


Fig (8): liver section of irradiated rat at 8 Gy (H&E×160).

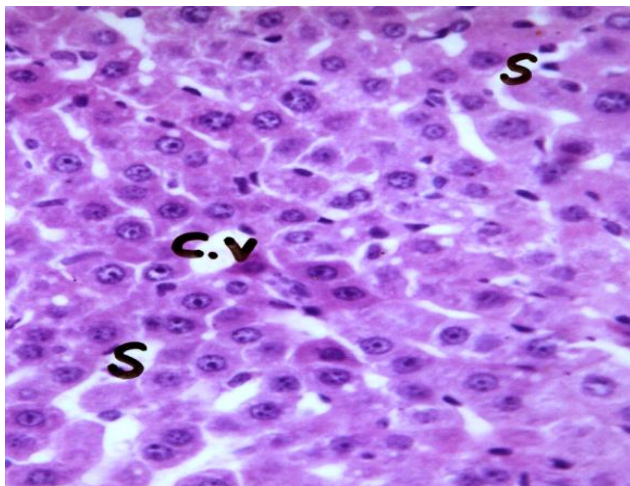


Fig (6): liver section of normal rat (H&E × 400)

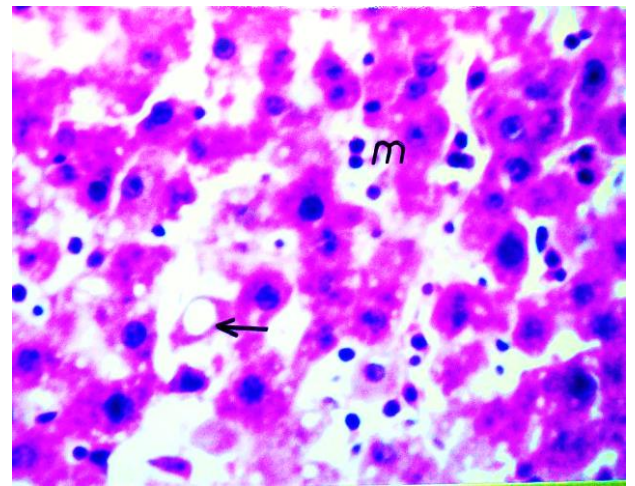


Fig (9): liver section of irradiated rat at 8 Gy (H&E×160).

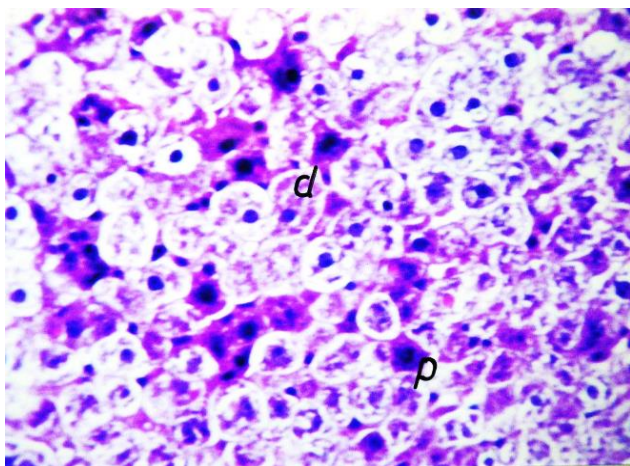


Fig (7): liver section of irradiated rat at 8 Gy (H&E×160)

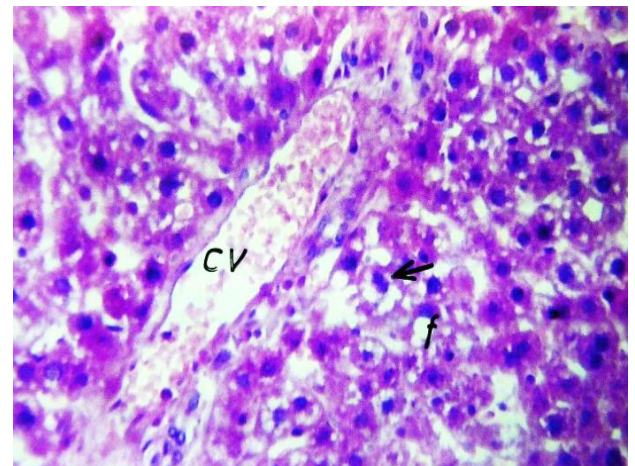
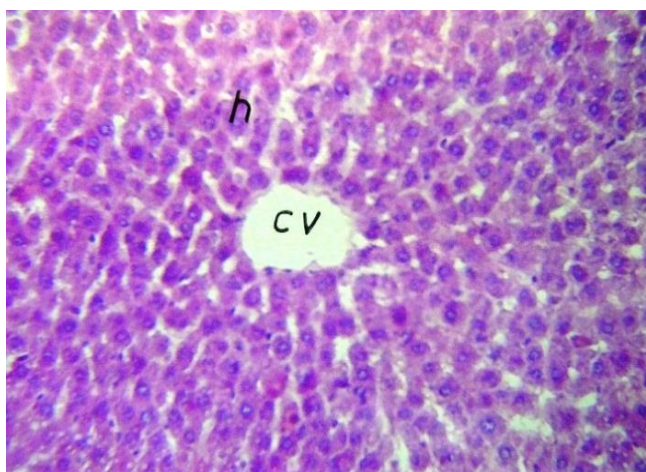
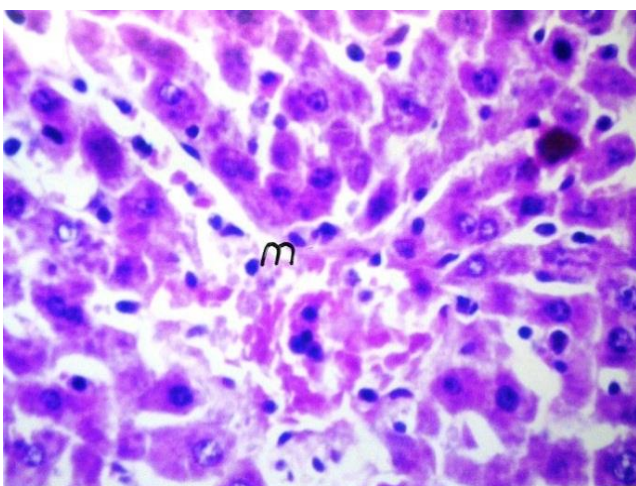


Fig (10): liver section of irradiated rat at 8 Gy (H&E×80).





**Fig (11):** liver section of irradiated rat at 8 Gy and treated by nAg/HAp (H&E×64).



**Fig (12):** liver section of irradiated rat at 8 Gy and treated by nAg/HAp (H&E×160).

## DISCUSSION

Radiation therapy represents an important status in the treatment of various types of cancer. However, a general view of radiation is damage to normal tissue due to interaction between the ROS build-up and organic tissue. This interaction leads to the damage of different components in the cell resulting in biochemical and histological changes [20]. The liver is a radiosensitive organ and exposure to irradiation can induce liver damage and can increase the risk of hepatic cancers [21].

In the current study, the damaging effect of irradiation on DNA is manifested by alterations of comet parameters. Comet assay is widely used to detect genotoxicity and cellular DNA lesions [22, 23, 24]. The main reasons of DNA damage are; direct action of radiation, which causes defect in the chemical bonds of

DNA structure leading to strand breaks and indirect action consequently to large production of ROS, caused various types of DNA damage [24, 25]. On the other hand, ROS attack DNA guanine bases produce formation of 8-OHdG, which can bind to thymidine rather than cytosine [25]. Thus, 8-OHdG is a reliable indicator for DNA oxidative damage and elevation of 8-OHdG in hepatic tissue in irradiated rats confirmed this hypothesis. Apoptosis is a hallmark cascade of irradiation due to direct hits the DNA molecule and change the molecular structure. Caspase-3 (executioner caspase), is activated during apoptotic pathway and plays a dominant role in coordination of the demolition phase of apoptosis by cleaving a varied array of protein substrates [26, 27]. The elevation of caspase -3 level in the irradiated group reflected the harmful effect of irradiation on molecular components of the cells.

The imbalance between oxidation and natural antioxidant systems can be executed by irradiation generated large amounts of ROS [28]. The obtained results showed a marked increase in MDA content accompanied with reduction in SOD, GPx and CAT concentrations in hepatic tissues of irradiated rats. It is well known that ROS is the major key of the broken balance between oxidant and antioxidant system [28, 29]. The increase of MDA content may reflect the high degree of lipid peroxidation in liver tissue and implies the failure of the antioxidant system in repulse the flood of ROS [29]. The depletion in the antioxidant enzymes in liver (SOD, GPx and CAT) is a rational result because the capability of these enzymes is insufficient to encounter ROS cascade and accompanied lipid peroxidation byproducts [30]. The increase in the concentration of MDA points to the extensive of oxidative stress, SOD neutralizes  $\bullet\text{O}_2^-$  by converting it to oxygen  $\text{O}_2$  and  $\text{H}_2\text{O}_2$ , and then,  $\text{H}_2\text{O}_2$  is converted to  $\text{H}_2\text{O}$  and  $\text{O}_2$  by the assistance of CAT [31].

Consequently, the functional capacity of liver tissue was impaired leading to an increase in the activities of serum transaminases (AST & ALT), LDH enzymes and TB as well as depletion in the level of Alb. Just the hepatocyte damage, the cell membrane permeability increases that facilitates the cytoplasmic enzymes leakage through the damaged membrane to the blood [32, 33]. Bilirubin is produced from the breakdown of hemoglobin and carried by albumin to the liver. Once, in the liver, it conjugates with glucuronic acid. This conjugation may be formed a mass hindrance and the unconjugated bilirubin is release into the blood stream from damaged hepatocytes leading to increment its level in serum [34]. The phenomenon of hypoalbuminemia



refers to alterations the incidence in gene metabolism results from proteomic damage and impaired its synthesis within extensive liver damage induced by irradiation [35]. Thus, the up regulation of bilirubin and down regulation of albumin in the serum of the irradiated rats is ascribed to the adverse effect of irradiation on hepatic cells.

Exposure to irradiation-mediated ROS inflicts a vast interplay of inflammatory response including activation of the expression of cytokines, stress-sensitive kinases and transcription factors [36]. The present study showed a significant increase in serum values of TNF- $\alpha$ , IL-6, IL-10, MCP-1 and MMP-9 in irradiated rats. TNF- $\alpha$  tightly coordinated pro-inflammatory cytokines activation such as IL-6, IL-10 and monocyte chemoattractant protein-1 (MCP-1) as well as MMP-9 by regulating the stimulation of T cell expression to secrete cytokines. IL-6 has a dual role, as a proinflammatory cytokine and as anti-inflammation regulator, which stimulates the anti-inflammatory cytokine such as IL-10 and certain liver-specific transcription factors [37, 38]. Likewise, IL-10 down regulates the activity of TNF- $\alpha$  and inhibits the production of IL-6 for long-term [39].

The battery of tests applied in the current study are important because the hepatic functions are not simultaneously affected and to confirm the potential therapeutic effect of nAg/HAp thus; the single parameter is not accurate to detect the liver disorder. The results showed a significant effect of nAg/HAp in the recovery of most of the molecular, biochemical and histological changes consequent to irradiation. The impact of nAg/HAp was more pronounced in inhibition of the oxidative stress associated with the repair of the fragmented DNA and a reduction of inflammatory cytokines with consequence of improvement in serum hepatic enzymes. Such findings were consistent with the results reported in previous studies [8, 40 & 41]. Some researchers suggested that nAg cytotoxicity is mainly attributed to the interaction of nAg with the biological media and release of Ag<sup>+</sup>. The most important cytotoxicity mechanism of nAg is the interaction of Ag<sup>+</sup> with sulfur containing macromolecules [5]. The study on lung carried by Cameron et al., [42] suggested that insoluble Ag<sub>2</sub>S reduces the potential toxicity of nAg because Ag<sub>2</sub>S complexes around nAg particles may act as Ag<sup>+</sup>-sequestering and inhibits the toxicity mechanism. However, there is no consensus on nAg toxicity because *in-vivo* studies carried out with short-term experiments or in *in-vitro* studies can not be applicable to living system [43]. In addition, some studies challenged that nAg induced ROS production

and based their results on the difference in experimental conditions such as treatment duration, cell types, the method used for ROS detection as well as factors contributed to nAg synthesis and the physicochemical characteristic of the final product [8,42,44]. The current study dealt with modifying the manufacture of nAg supported on nHAp in order to examine the efficiency of this nanocomposite against the hazardous effect of radiation exposure. The nanocomposite of Ag/HAp contains low content of Ag nanoparticle (1/5 LD<sub>50</sub>) and has been prepared by the chemical route and subsequent chemical neutralization process. In this method, Polyvinyl alcohol (PVA) is used to act as a polymeric matrix where Ag ions are distributed on it to form a crystalline structure in nano range as the same as Ca ions without agglomeration. The prevailing view is that the oxidative stress accompanied with ROS has a complete responsibility for any damage at cellular or systemic level occurring from either extrinsic or intrinsic conditions [8, 9, 32]. The current results showed inhibition of lipid peroxidation products represented by decrease of hepatic MDA level and activation of antioxidant enzymes elevation of hepatic GPx, SOD and CAT concentrations. Such results are in line with previous studies by Hassen et al., [34] and Antony et al., [45] who revealed that nAg decreased the level of NO when utilized in the treatment of hepatocarcinoma and others found no change in ROS level after nAg administration [42,46 & 47]. The current study showed that nAg/HAp i.v. injection ameliorated the liver function biomarkers and this finding may be attributed to changing the integrity and permeability of hepatocytes membrane. Such findings agreed with the results of Hassen [34], Singh et al., [41] and Melo et al., [48] who reported that there was a significant decrease in aminotransaminases and bilirubin level after nAg treatment that may be attributed to normal regeneration of liver activity. The down stimulation of inflammatory cytokines was tightly associated with less oxidative stress. Injection of nAg/HAp decreases the induction of cytokines that may be due to minimizing oxidative destruction mechanism mediated ROS to the liver cells other than evoking the activity of antioxidant enzymes [49]. Although, nAg/HAp can be a potential in medical applications because the formulation structure is a combination from biocompatible and antibacterial materials, the studies conducted on this nanocomposite are rare. Previously, Inderand Kumar [4] suggested that, it is important to standardize the formulation of nAg to avoid the potential toxicity and with each combination with other particle; the composite is being utilized to

produce nanoparticles with unique physiochemical properties, controlled size and shape of particles.

The effective role of nAg/HAp in repairing the fragmented DNA and in ameliorating the liver related-biochemical markers were confirmed by hepatic histopathological features. Hence, the examination of liver sections from IR+nAg/HAp rats showed a complete disappearance of severe histopathological changes induced by irradiation with few inflammatory cells diffusing between the hepatocytes.

## CONCLUSIONS

A composite of nAg successfully dispersed into nHAp matrix was synthesized by a chemical route to produce a final biosafe product (nAg/HAp). The nanoparticles were supported on a matrix and nHAp trapped nAg to control the release of Ag<sup>+</sup> in biological media. The prepared nanocomposite with its physiochemical characteristics effectively ameliorate the hepatocytes damage induced by exposure to 8 Gy  $\gamma$ -irradiation. According to the molecular, biochemical and histopathological results, nAg/HAp represents a potential effect to a high degree in recovering the serious effect following exposure to irradiation and thus, represents a prospective treatment for such cases.

## Declaration of Competing Interest:

The authors reported no potential conflict of interest

## REFERENCES

- [1] Yin, I.X., Zhang, J., Zhao, I.S., Mei, M.L., Li, Q. and Chu, C.H. (2020). The Antibacterial Mechanism of Silver Nanoparticles and Its Application in Dentistr. *Int. J. Nanomed.* **15**, 2555-2562.
- [2] Singh, R. and Nalwa, H.S. (2011). 'Medical applications of nanoparticles in biological imaging, cell labeling, antimicrobial agents, and anticancer nanodrugs'. *J. Biomed. Nanotech.* **7**, 489-503.
- [3] Mahakalkar, A. and Hatwar, B. (2014). 'Biophysicochemical Characteristics & Applications of Nanoparticles: Mini Review'. *Am. J. Drug Deliv. Ther.* **1**, 035-041.
- [4] Inder, D. and Kumar, P. (2018). The Scope of Nano-Silver in Medicine: A Systematic Review. *Int. J. Pharmacogn. Chinese Med.* **2** (2).
- [5] McShan, D., Ray, P.C. and Yu, H. (2014). Molecular Toxicity Mechanism of Nanosilver. *J. Food Drug Anal.* **22**(1), 116–127.
- [6] Oliveira, M.M., Ugarte, D., Zanchet, D. and Zarbin, A.J.G. (2005). Influence of synthetic parameters on the size, structure, and stability of dodecanethiol-stabilized silver nanoparticles. *J. Colloid Interface Sci.* **292**(2), 429-35.
- [7] Korbekandi, H. and Iravani, S. (2012). Silver Nanoparticles, IN: The Delivery of Nanoparticles, Hashim, A. A. Ed. Intech, and Rijeka, Croatia 2012: .Page 3.
- [8] Abdel-Gawad, E.I., El-Sherbiny, E.M., and Awwad, S.A. (2021). New synthesis for nano-silver formulated as a bio-safe composite structure to employ against hepatotoxicity in rats. *Frontiers in Drug. Chem. Clin. Res.* **4**, 1-8.
- [9] Abdel-Gawad, E.I., and Awwad, S.A. (2018). The devastating effect of exposure to high irradiation dose on liver and the performance of synthesized nano-Hap in relieve the associated symptoms in rats. *Biochem. Cell Biol.* **96** (5), 507–514.
- [10] Hei, T.K., Zhou, H., Chai, Y., Ponnaiya, B., Vladimir, N. and Ivanov, V. (2011). Radiation Induced Non-targeted Response: Mechanism and Potential Clinical Implications. *Curr. Mol. Pharmacol.* **4**(2), 96–105.
- [11] Lorke, D. (1983). A new approach to practical acute toxicity testing. *Arch. Toxicol.* **54**(4), 275-287.
- [12] Guide for the Care and Use of Laboratory Animals, 8th edition. (2011). National Research Council (US) Committee for the Update of the Guide for the Care and Use of Laboratory Animals. Washington (DC): National Academies Press (US); 2011.
- [13] Erdelmeier, I. (1997). Reactions of N-methyl-2-phenylindole with malondialdehyde and 4-hydroxyalkenals. Mechanistic aspects of the colorimetric assay of lipid peroxidation. *Chem. Res. Toxicol.* **11**, 1184–1194.
- [14] Janknegt, P.J., Rijstenbil, J.W., van de Poll, W.H., Gechev, T.S. and Buma, A.G.J. (2007). A comparison of quantitative and qualitative superoxide dismutase assays for application to low temperature microalgae. *J. Photochem. Photobiol.B, Biol.* **87**, 218–226.
- [15] Paglia, D.E. and Valentine, W.N. (1967). Studies on the Quantitative and Qualitative Characterization of Erythrocyte Glutathione Peroxidase. *J. Lab. Clin. Med.* **70**, 158-169.
- [16] Aebi, H. (1984). Catalase in vitro. *Methods Enzymol.* **105**, 121-126.

- [17] German Society for Clinical Chemistry. (1970). Standardization of methods for the determination of enzyme activities in biological fluids. *J. Clin. Chem. Clin. Biochem.* **8**, 658-660.
- [18] Vanderlinde, R.E. (1985). Measurement of total lactate dehydrogenase activity. *Ann. Clin. Lab. Sci.* **15**, 13-31.
- [19] Bancroft, J.D. and Stevens, A. Foreword by Turner, D.R, (2008). Theory and practice of histological techniques. (6th ed. New York, Churchill Livingstone, USA). 121.
- [20] Cheng, W., Xiao, L., Ainiwaer, A., Wang, Y., Wu, G., Mao, R., Yang, Y. and Bao, Y. (2015). Molecular Responses Of Radiation-Induced Liver Damage In Rats. *Mol. Med. Rep.* **11**(4), 2592–600.
- [21] Shahid, S., Masood, K. and Khan, A.W. (2021). Prediction of impacts on liver enzymes from the exposure of low-dose medical radiations through artificial intelligence algorithms. *Rev. Assoc. Med. Bras.* **67** (2), 248-259.
- [22] Tiwari, P., Kumar, A., Balakrishnan, S., Kushwaha, H.S. and Mishra, K.P. (2009). Radiation-Induced Micronucleus Formation And DNA Damage In Human Lymphocytes And Their Prevention By Antioxidant. *Thiols. Mutat. Res.* **676**, 62–68.
- [23] Nandhakumar, S., Parasuraman, S., Shanmugam, M.M., Rao, K.R., Chand, P. and Bhat, B.V. (2011). Evaluation of DNA damage using single-cell gel electrophoresis (Comet Assay). *J. Pharmacol. Pharmacother.* **2**(2), 107-111.
- [24] Uslu, H., Uslu, G.A., Özen, H. and Karaman, M. (2018). Effects of different doses of *Prunus laurocerasus* L. leaf extract on oxidative stress, hyperglycaemia and hyperlipidaemia induced by type I diabetes. *Indian J. Tradit. Knowl.* **17**(3), 43-436.
- [25] Liu, C., Liao, K., Gross, N., Wang, Z., Li, G., Zuo, W., Zhong, S., Zhang, Z., Zhang, H., Yang, J. and Hu, G. (2020). Homologous recombination enhances radioresistance in hypopharyngeal cancer cell line by targeting DNA damage response. *Oral Oncol.* **100**, 104469.
- [26] D'Amelio, M., Cavallucci, V. and Cecconi, F. (2010). Neuronal Caspase-3 Signaling: Not Only Cell Death. *Cell. Death. Differ.* **17**, 1104–14.
- [27] Jones, J.R., Kong, L., Hanna, M.G.I.V., Hoffman, B., Krencik, R., Bradley, R., Hagemann, T., Choi, J., Doers, M., Marina Dubovis, M., Sherafat, M.A., Bhattacharyya, A., Christina Kendzioriski, C., Audhya, A., Messing, A. and Zhang, S. (2018). Mutation In Dgfp Disrupt The Distribution And Function Of Organelle In Humanastrocytes. *Cell. Report.* **25**, 947–958.
- [28] Pan, C.C., Kavanagh, B.D., Dawson, L.A., Li, X.A., Das, S.K., Miften, M. Ten Haken, R.K. (2010). Radiation-Associated Liver Injury. *Int. J. Radiat. Oncol. Biol. Phys.* **76**(3), 94–100.
- [29] Xie, L.H., Zhang, X., Hu, X., Min, X., Zhou, Q. and Zhang, H. (2016). Mechanisms of an Increased Level of Serum Iron in Gamma-Irradiated Mice. *Radiat. Environ. Biophys.* **55**, 81–88.
- [30] Abdelhalim, M.A., and Moussa, S. (2013). The biochemical changes in rats' blood serum levels exposed to different gamma radiation doses. *Afr. J. Pharm. Pharmacol.* **7**(15), 785-792.
- [31] Li, Q., Qiu, Z., Wang, Y., Guo, C., Cai, X., Zhang, Y., Liu, L., Xue, H. and Tang, J. (2021). Tea Polyphenols Alleviate Hydrogen Peroxide-Induced Oxidative Stress Damage Through The Mst/Nrf2 Axis And The Keap1/Nrf2/HO-1 Pathway In Murine RAW264.7 Cells. *Exp. Ther. Med.* **22**, 1473.
- [32] Peixoto, A., Pereira, P., Bessa De Melo, R. and Macedo, G. (2017). Radiation-Induced Liver Disease Secondary to Adjuvant Therapy for Extra-Hepatic Cholangiocarcinoma. *Dig. Liver Dis.* **49**(2), 227.
- [33] Abou Zeid, S.M., EL-Bialy, B. E., EL-Borai, N. B., Abubakr, H.O. and Elhadary A. (2018). Radioprotective Effect of Date Syrup on Radiation-Induced Damage in Rats. *Sci. Rep.* **8**:7423.
- [34] Hassen, M.T., Ahmed, N.J. and Mohamed, H.K. (2020). Therapeutic Effect Of Silver Nanoparticles Against Diethyl Nitrosamin And Carbon Tetrachloride-Induced Hepatocellular Carcinoma In Rats. *Int. J. Pharm. Pharm. Sci.* **12**(9), 0975-1491.
- [35] Jiang, L., Jia ,H., Tang , Z., Zhu , X., Cao , Y., Tang ,Y., Yu , H., Cao ,J., Zhang , H. and Zhang, S. (2019). Proteomic Analysis of Radiation-Induced Acute Liver Damage in a Rabbit Model. *Dose-Response.* **17**(4), 1559325819889508.
- [36] Dent, P., Yacoub, A., Contessa, J., Caron, R., Amorino, G., Valerie, K., Hagan, M.P., Grant, S. and Schmidt-Ullrich, R. (2003). Stress and radiation-induced activation of multiple



- intracellular signaling pathways. *Radiat. Res.* **159** (3), 283-300.
- [37] Zhang, L., Van Handel, M., Schartner, J.M., Hagar, A., Allen, G., Curet, M. and Badie, B. (2007). Regulation of IL-10 expression by upstream stimulating factor (USF-1) in glioma-associated microglia. *J. Neuroimmunol.* **184**, 188-197.
- [38] Porta, C., De Amici, M., Quaglini, S., Paglino, C., Tagliani, F., Boncimino A, Moratti, A. and Corazza, G. R. (2008). Circulating Interleukin-6 As A Tumor Marker For Hepatocellular Carcinoma. *Ann. Oncol.* **19**, 353- 358.
- [39] Brkic, M., Balusu, S., Libert, C., Roosmarijn, E. and Vandenbroucke, R.E. (2015). Friends or Foes: Matrix Metalloproteinases and Their Multifaceted Roles In Neurodegenerative Diseases. *Mediators Inflamm.* (2015) Article ID 620581, 27 Pages.
- [40] Gallorini M., di Giacomo V., Di Valerio V., Rapino M., Bosco D., Travan A., Di Giulio M., Di Pietro R., Paoletti S., Cataldi A. and Sancilio S. (2016). Cell-protection mechanism through autophagy in HGFs/S. mitis co-culture treated with Chitlac-nAg. *J. Mater. Sci. Mater. Med.* **27**, 186.
- [41] Singh, A., Darb, M.Y., Joshic, B., Sharmac, B., Shrivastavaa, S. and Shukla, S. (2018). Phytofabrication of Silver nanoparticles: Novel Drug to overcome hepatocellular ailments. *Toxicol. Rep.* **5**, 333–342.
- [42] Cameron, S.J., Hosseinian, F. and Willmore, W.G. (2018). A current overview of the biological and cellular effects of nanosilver. *Int. J. Mol. Sci.* **19**(7), 2030.
- [43] Ge, L., Li, Q., Wang, M., Ouyang, J., Li, X. and Malcolm MQ Xing, M.M.Q. (2014). Nanosilver Particles in Medical Applications: Synthesis, Performance, and Toxicity. *Int. J. Nanomedicine.* **9**, 2399–2407.
- [44] Pereira, L.C., Pazin, M., Franco-Bernardes, M.F., da Cunha Martins, Jr.A., Barcelos, G.R.M., Pereira, M.C., Mesquita, J.P., Rodrigues, J.L., Barbosa, Jr.F. and Dorta, D.J. (2018). A perspective of mitochondrial dysfunction in rats treated with silver and titanium nanoparticles (AgNPs and TiNPs). *J. Trace Elem. Med.* **47**, 63–69.
- [45] Antony, J.J., Sithika, M.A.A., Joseph, T.A., Suriyakalaa, U., Sankarganesh, A., Siva, D., Kalaiselvi, S. and Achiraman, S. (2013). In vivo antitumor activity of biosynthesized silver nanoparticles using *Ficus religiosa* as a nanofactory in DAL induced mice model. *Colloids Surf., B: Biointerfaces.* **108**, 185-190.
- [46] Wang, Z., Liu, S., Ma, J., Qu, G., Wang, X., Yu, S., He, J., Liu, J., Xia, T. and Jiang, G.B. (2013). Silver nanoparticles induced RNA polymerase-silver binding and RNA transcription inhibition in erythroid progenitor cells. *ACS Nano.* **7**(5), 4171–4186.
- [47] Chen, Y., Wang, Z., Xu, M., Wang, X., Liu, R., Liu, Q., Zhang, Z. H., Xia, T., Zhao, J.C., Jiang, G.B., Xu, Y. and Liu, S.J. (2014). Nanosilver incurs an adaptive shunt of energy metabolism mode to glycolysis in tumor and nontumor cells. *ACS Nano.* **8** (6), 5813–5825.
- [48] Melo, P.S., Marcato, P.D., Huber, S.C., Ferreira, I.R., De Paula, L.B., Almeida, A.B.A., Durán, N., Torsoni, S., Seabra, A.B. and Alves, O.L. (2011). Nanoparticles In Treatment Of Thermal Injured Rats: Is It Safe? *J. Phys.: Conf. Ser.* **304**, 012027:1-8.
- [49] Aboubakr, E.M., Taye, A., Aly, O.M., Gamal-Eldeen, A.M. and El-Moselhy, M.A. (2017). Enhanced anticancer effect of combretastatin A-4 phosphate when combined with vincristine in the treatment of hepatocellular carcinoma. *Biomed. Pharmacother.* **89**, 36-46.